

NONTHERMAL ELECTRON-POSITRON PAIRS AND THE BREAK IN THE HARD X-RAY SPECTRUM OF NGC 4151

PAOLO S. COPPI

Department of Astronomy and Astrophysics, University of Chicago, 5640 South Ellis Avenue, Chicago, IL 60637

AND

ANDRZEJ A. ZDZIARSKI

N. Copernicus Astronomical Center, Bartycka 18, PL-00-716 Warsaw, Poland¹

Received 1992 March 17; accepted 1992 July 28

ABSTRACT

The recent observation by the detectors on board *GRANAT* of a spectral steepening above ~ 50 keV imposes a constraint on possible emission models for NGC 4151. This steepening, for example, is not well fitted by an exponential rollover characteristic of a purely thermal model, or by a Compton-downscattered power law. We find that this spectral behavior is consistent with that produced by a photon-starved non-thermal pair plasma with high compactness. This is the first quantitative test of the nonthermal pair plasma model against broad-band X-ray/ γ -ray observations. Above 200 keV or so, the nonthermal pair plasma model predicts an upturn in the spectrum, and a thermal annihilation feature around 511 keV. Such spectral behavior should be looked for with *GRO*.

Subject headings: galaxies: individual (NGC 4151) — radiation mechanisms:
 Compton and inverse Compton — X-rays: galaxies

1. INTRODUCTION

NGC 4151 is a nearby, low-luminosity Seyfert galaxy. Its redshift of $z = 0.0033$ corresponds to a distance of 20 Mpc at $H_0 = 50 \text{ km s}^{-1} \text{ Mpc}^{-1}$. Its X-ray luminosity in the 2–10 keV range varies from 0.3×10^{43} to $2 \times 10^{43} \text{ ergs s}^{-1}$. The energy spectral index in the 2–10 keV range is $\alpha \approx 0.5 \pm 0.2$ (Yaqoob & Warwick 1991). The X-ray spectrum above 10 keV was relatively stable for several years, with a spectral index roughly equal to the average 2–10 keV index. Specifically, α was 0.50 ± 0.27 in the 30–80 keV range in 1986 (Perotti et al. 1990), 0.54 ± 0.09 in the 15–200 keV range in 1987 (Perotti et al. 1991), and 0.54 ± 0.11 in the 20–100 keV range in 1987–1989 (Maisack et al. 1989).

In 1990 November, NGC 4151 was observed nearly simultaneously in the 3–30 keV range by the ART-P detector (Apal'kov et al. 1992) and in the 40–10³ keV range by the SIGMA detector (Jourdain et al. 1992, hereafter J92), both on board the *GRANAT* satellite. In marked contrast to the 1986–1989 observations, a distinct break was seen in the hard X-ray spectrum around 50 keV. The energy spectral index was $\alpha = 0.44 \pm 0.03$ below the break (Apal'kov et al. 1992) and $\alpha = 2.1_{-0.9}^{+1.1}$ above the break (J92). A spectrum consistent with this was observed twice before, by *HEAO 1* in 1978 June (Baity et al. 1984) and by *Einstein* and MISO in 1980 May (Bassani et al. 1986).

We explain here the two types of the X-ray spectra observed from 1986 to 1990 by the nonthermal e^\pm pair model (e.g., Zdziarski & Lightman 1985; Svensson 1987, hereafter S87; Lightman & Zdziarski 1987, hereafter LZ87) with a Compton reflection component (Zdziarski et al. 1990b, hereafter Z90b). In this model, energetic electrons or e^\pm pairs are injected at a large Lorentz factor, γ_i , into a compact region above some nearby cold ($kT \sim 10^5$ K) matter, e.g., an accretion disk. The

UV photons from the adjacent matter get Compton-upscattered by the injected pairs/electrons. For large enough γ_i , some of the upscattered photons have energies extending above the threshold for production of secondary e^\pm pairs in photon-photon collisions. The secondary pairs also Compton-upscatter photons, initiating an electromagnetic cascade (see S87 and Svensson 1992 for more discussion).

Because of the high photon density, the pairs lose most of their energy before they can escape the source region and thus form a thermal component with a temperature, T , determined by the balance of radiative gains and losses. The thermal pairs can have a substantial Thomson optical depth, $\tau_T > 1$, which is determined by the balance between pair production and pair annihilation. The thermal pairs also Compton-scatter photons present in the source, and their annihilation gives rise to a spectral feature near 511 keV.

A fraction of the radiation from the plasma is intercepted by the nearby cold matter and is reprocessed. Most of the radiation reemerges at much lower (UV) energies, but a fraction ($\sim 10\%$ – 20%) is Compton-scattered back into the line of sight, providing an additional hard X-ray component which peaks at several tens of kilo-electron volts. (See Pounds et al. 1990 and Z90b for a discussion of Compton reflection in Seyfert galaxies.) As discussed in Zdziarski (1992) and Svensson (1992), this reprocessing of the ambient radiation field by the e^\pm pair plasma and the adjacent matter appears to explain the properties of the ~ 0.5 – 30 keV spectra seen in the majority of nearby active galactic nuclei (AGNs).

For NGC 4151 we require the pair plasma to be “photon-starved.” In this case, the power in the injected particles, L_h , is much larger than the luminosity in soft (UV) photons, ΔL_s , intercepted by the nonthermal source (Zdziarski & Lamb 1986; Zdziarski, Coppi, & Lamb 1990a, hereafter Z90a). Here L_s is the total UV luminosity emitted by the AGN. As most of the power injected in the nonthermal particles is eventually radiated in hard photons, L_h is approximately equal to the

¹ Work done in part at the Massachusetts Institute of Technology, NASA/Goddard Space Flight Center, and Johns Hopkins University.

AGN luminosity in X-rays and γ -rays. As $L_s \sim L_h$ observationally, $\Delta \ll 1$ is required, which implies that the area subtended by the nonthermal source must be much less than the area of the UV source. Instead of L_h and L_s , it is often more convenient to use the dimensionless compactness parameters, l_h and l_s (e.g., S87). For nearly isotropic sources with a characteristic size R , the parameters are defined as

$$l_h \equiv \frac{L_h}{R} \frac{\sigma_T}{m_e c^3} \simeq \frac{L_h/R}{4 \times 10^{28} \text{ ergs s}^{-1} \text{ cm}^{-1}}, \quad l_s \equiv \frac{\Delta L_s}{R} \frac{\sigma_T}{m_e c^3}, \quad (1)$$

where σ_T is the Thomson cross section and m_e is the electron mass.

The condition of $l_s \ll l_h$ for NGC 4151 is imposed by the value of the spectral index of $\alpha < 0.5$ below ~ 10 keV. If $l_s \gtrsim l_h$, the first-order Compton scattering by nonthermal pairs dominates, which causes the X-ray spectral index to be always greater than 0.5, and to substantially exceed that value for $l_h \gtrsim 1$ (S87; LZ87). X-ray spectral indices less than 0.5 in the photon-starved case are obtained from *repeated* Compton upscattering, mostly by the thermalized pairs.

2. SPECTRAL MODELS

2.1. The Nonthermal Pair Model

We explain here the transient nature of the break at ~ 50 keV by a change in the compactness parameter l_h . For $l_h \gtrsim 10^2$, the Thomson optical depth of the thermal pairs is large, $\tau_T \simeq (l_h/10)^{1/2} \gg 1$ (S87; LZ87), which causes Compton scattering by thermal pairs to be important. We find that the combined effects of Compton upscattering, downscattering, and reflection satisfactorily explain the observed break in the 1990 spectral data. On the other hand, for $l_h \ll 10^2$, τ_T is small and the emitted spectrum can be close to a single power law up to hard X-ray energies (LZ87; Z90a). The low compactness state can explain the spectrum observed in 1986–1989.

Figure 1 presents an example of the nonthermal pair/

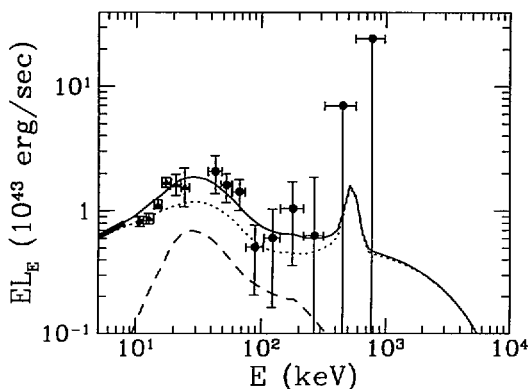


FIG. 1.—Fit of the pair/reflection model (solid curve) to the NGC 4151 X-ray spectrum in 1990 November. Triangles and circles represent the data from ART-P and SIGMA (J92), respectively. The heavy solid line below 10 keV is the best-fit power law to the ART-P data, with $\alpha = 0.44$ (Apal'kov et al. 1992). That power law gives the spectrum emitted by the source *before* absorption by intervening matter (which is not included in our model). The vertical axis gives the spectral luminosity per logarithmic photon energy interval. The model parameters are $l_h = 170$, $l_s = 8.8$, $\gamma_i = 100$, and $kT_s = 13$ eV. The reflection contribution (dashed curve) corresponds to 50% of the pair emission incident on neutral cold matter. The direct pair emission is shown by the dotted curve. One sees that the fit is satisfactory.

reflection spectrum (solid curve) compared with the ART-P/SIGMA 1990 data (as given in J92). The model spectrum has been obtained using the code described in Coppi & Blandford (1990) and Coppi (1992; tested against the code of LZ87), and including reflection from a flat disk subtending a 2π solid angle (Lightman & White 1988; Z90b). The main parameters of the model shown are $l_h = 170$ and $l_h/l_s = 19.3$.

The energy distribution of background UV photons intercepted by the plasma was assumed to be a diluted (by some factor $f \leq 1$) blackbody with temperature T_s . We note that T_s is determined by the other model parameters. This follows from setting fL_s , as obtained from the blackbody formula, equal to that obtained from the observed L_h and the fitted values of l_h and l_h/l_s (see eq. [1]). We find T_s weakly dependent on f (expected to be $\ll 1$ in photon-starved plasmas),

$$kT_s \simeq 1.5 h^{1/2} (l_s l_h f)^{1/4} \text{ eV}, \quad (2)$$

where $h \equiv H_0/(50 \text{ km s}^{-1} \text{ Mpc}^{-1})$, and the projected area of the source was assumed to equal πR^2 . We use here the approximately self-consistent value of $kT_s = 13$ eV.

For the model of Figure 1, the parameters of the thermal plasma component are $kT = 9.9$ keV and $\tau_T = 5.8$. The Compton parameter (e.g., Rybicki & Lightman 1979) is then $y = 4(kT/m_e c^2)(\tau_T^2/2) \simeq 1$. This implies that the original nonthermal spectrum is strongly upscattered up to the peak energy of $3kT \simeq 30$ keV. On the other hand, nonthermal photons at higher energies, E , undergo $\sim \tau_T^2/2$ scatterings with a fractional energy decrease per scattering of $-E/m_e c^2$. The product of these two quantities is the analog of the Compton y -parameter for downscattering and reaches unity at $2m_e c^2/\tau_T^2 \simeq 31$ keV, where a spectral break is formed (Sunyaev & Titarchuk 1980, hereafter ST80). We see that the expected break energies for both thermal upscattering and downscattering nearly coincide, giving rise to the strongest break possible in the model. In addition, the Compton reflection component peaks at a few tens of keV, further increasing the break at higher energies. Note that Compton upscattering by the thermal plasma of UV seed photons alone would produce an X-ray spectrum with $\alpha \sim 1$, which is much softer than the observed one. The reason for obtaining the much harder X-ray spectrum is that the thermal plasma upscatters the broad distribution of nonthermally produced photons.

After breaking around 30 keV, the model spectrum gradually flattens above 100 keV due to the Klein-Nishina reduction of the Compton cross section, which reduces the number of scatterings with thermal pairs experienced by a high-energy photon. The spectrum contains a thermal annihilation feature around 511 keV (Zdziarski 1980; Svensson 1983). The feature is well below the SIGMA upper limits. One sees that the model agrees well with the data, with the model spectrum going through almost all error boxes.

Figure 2 compares the nonthermal pair/reflection model with the *Ginga*/HEXE 1987 November data (Maisack & Yaqoob 1991). This state of NGC 4151 is compatible with other observations from 1986 to 1989 (see § 1). The main parameters of the model are $l_h = 40$, and $l_h/l_s = 20$ (approximately the same as for Fig. 1). We again see that the model agrees well with the data.

We find that the presence of the reflection component is consistent with both data sets. We also find that it improves the fit for the 1990 data and allows l_h/l_s to be relatively small (which imposes less severe constraints on the source geometry)

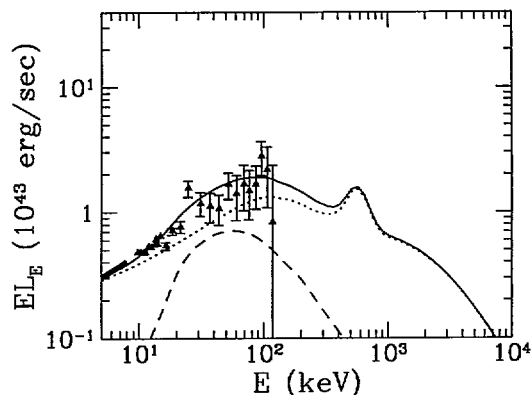


FIG. 2.—Fit of the pair/reflection model to the NGC 4151 X-ray spectrum in 1987 November. The triangles and the heavy solid line below 10 keV represent the combined *Ginga*/HEXE data and a best power-law fit (with $\alpha = 0.37$) to the data, respectively. The curves correspond to the spectral components analogous to those in Fig. 1. The model parameters different from those in Fig. 1 are $l_h = 40$, $l_s = 2$, $\gamma_i = 56$. One sees that the fit is satisfactory.

and roughly constant from 1987 to 1990, which allows for the interpretation of the spectral variability as a correlated change in the source compactness due to a change in the source size (see below).

Our conclusion that the presence of the reflection component is allowed may appear to conflict with the results of Maisack & Yaqoob (1991). They found that such a component is not compatible with the 1987 *Ginga*/HEXE data. However, their conclusions are valid only when the incident spectrum is a pure, unbroken power law. In our model, the incident spectrum is not a power law (it rolls over above ~ 100 keV), and reflection is then allowed.

Since we did not have the response matrices of the detectors, we did not attempt to find the minimum χ^2 model fit to the data. The purpose of this *Letter* is to point out that the non-thermal pair model can provide a reasonable fit to the data. A systematic search of the model parameter space using the instrumental response functions would be very useful. In such a search, one could also take into account constraints on the reflection component from other considerations (e.g., from the strength of the Fe $K\alpha$ line; Weaver et al. 1992). For the case where the allowed reflection contribution is small, we find that the nonthermal pair model still appears able to fit the 1990 data. However, the source must then be very photon-starved, with $l_h/l_s \gg 20$. This imposes stringent constraints on the source geometry.

We have shown the expected γ -ray spectra in the 1–10 MeV range in Figures 1 and 2. These are only rough estimates, since the amplitude of the spectrum above 1 MeV is sensitively (positively) correlated with the value of γ_i , e.g., the maximum energy in the spectrum is $\sim 0.5\gamma_i$ MeV.

The model bolometric luminosity from soft X-rays to γ -rays is almost the same for the two cases, $L_h \simeq (7-8) \times 10^{43}$ ergs s^{-1} . Because we assumed l_h/l_s to be constant, the luminosity in the soft UV photons incident on the nonthermal source, ΔL_s , has also to be constant. If the nonthermal source is approximately spherical, the increase of l_h from 1987 to 1990 requires a reduction of the size R . This in turn requires an increase in the UV flux incident on the nonthermal source to compensate for the reduction of R . This can be achieved either by a correlated decrease in the size of the UV source or by an increase of L_s . The latter is, in fact, indicated by the observations of Ayani & Maehara (1991).

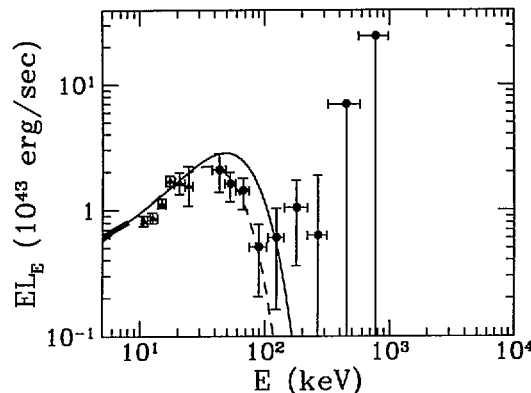


FIG. 3.—Attempts to fit the ART-P/SIGMA data using a thermal Comptonization model (ST80). The dashed and solid curves show the spectra obtained for $kT_e = 11$ keV, $\tau_T = 9.38$, and $kT_e = 15$ keV, $\tau_T = 7.94$, respectively. The spectra are independent of the temperature of seed photons, T_s , provided that $kT_s \ll 1$ keV. One sees that this model provides a worse fit to the data than the model of Fig. 1.

2.2. Alternative Models

We have tested two alternative models against the ART-P/SIGMA data. Figure 3 shows our results for the pure thermal model, in which the spectrum is due to repeated Compton scatterings of the seed photons by a thermal plasma cloud with large optical depth. To produce the spectra shown, we have used the results of ST80. We see that the dashed curve fits well the points below 100 keV, but it falls much below the points at higher energies. On the other hand, the fit going through the point at 120 keV (solid curve) is much above the points at lower energies. The same is the case for a thermal fit going through the 180 keV point. Thus, the 120 and 180 keV detection points require the presence of an extra component at high energies. Although the two points are only about 2σ detections, their combined presence is of about 3σ significance. Thus, while the thermal model probably cannot be excluded on the basis of the data, it appears to provide a significantly worse fit than the pair/reflection model.

We have also tested the model in which a power-law spectrum is transmitted through a fully ionized slab with large Thomson optical depth τ_T . One can then obtain a break due to Compton downscattering, as discussed above. From Figure 4

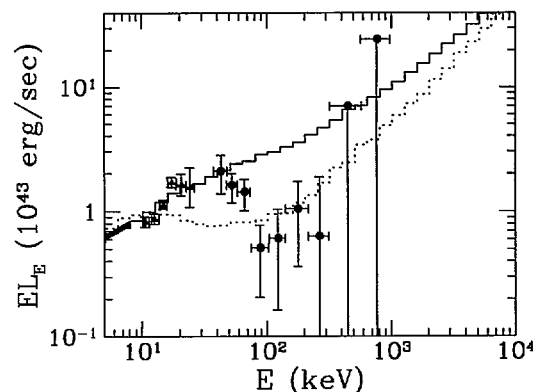


FIG. 4.—Attempts to fit the ART-P/SIGMA data by a power-law spectrum Compton-downscattered in crossing a slab of fully ionized nonrelativistic electrons. The incident power law has a spectral index equal to the best-fit ART-P spectral index, $\alpha = 0.44$. The solid histogram shows the resulting spectrum for a slab optical depth $\tau_T = 3$; the dashed histogram, that for $\tau_T = 8$. One sees that no good fit can be obtained with this model.

we see that downscattering by itself is not sufficient to explain the break in the SIGMA data. The histograms are the transmission spectra obtained by the Monte Carlo method, using the code of White, Lightman, & Zdziarski (1988). The solid histogram corresponds to $\tau_T = 3$, for which the break occurs at the right energy but is then much too shallow. The dotted histogram corresponds to $\tau_T = 8$, for which the depression in the transmitted spectrum around 100 keV is compatible with the data. However, the break energy is then around 10 keV, in strong disagreement with the data.

3. DISCUSSION

We have shown that the nonthermal photon-starved pair/reflection model can explain the steep spectral break at ~ 50 keV seen in the 1990 observation of NGC 4151 by instruments on board *GRANAT*. The model can also explain the 1986–1989 spectral state of NGC 4151, in which the spectrum is a single power law up to $\sim 10^2$ keV. The combined results of ART-P and SIGMA and of *Ginga* and HEXE, which span two to three decades in photon energy, have allowed for the first time a quantitative test of the broad-band spectral predictions of the nonthermal pair/reflection model. We note that tests over a more restricted energy range, e.g., matching the observed 2–10 keV spectral index, are not as useful, since there are often several mechanisms capable of producing the spectral indices seen in this and other AGNs.

Our conclusions agree with those of Yaqoob (1992, hereafter Y92), who tested the nonthermal pair model by combining 2–10 keV X-ray spectra of NGC 4151 with the variability data on short time scales. He showed that a (photon-starved) model similar to ours explains the positive correlation between the spectral index and flux seen by *EXOSAT* and *Ginga*. The values of l_h/l_s , and of l_h for 1989 observations obtained by us lie within the corresponding ranges found by Y92, while the value of l_h obtained for 1990 observations is above his maximum value. His model did not include reflection, which is marginally

important in the 2–10 keV range. Adding reflection has the effect of increasing the fitted values of l_h (Z90b), which would then improve the agreement between our results and those of Y92.

The minimum X-ray flux-doubling variability time scale for NGC 4151 is a few times 10^4 s (Yaqoob & Warwick 1991). This implies a lower limit on the compactness of $l_h \gtrsim 2$, which is compatible with the pair models presented here.

We point out, however, that our model cannot explain the very strong γ -ray flux around 1 MeV seen in 1977 by MISO (Perotti et al. 1979), as well as an upturn in the spectrum above 200 keV seen in 1987 by MIFRASO (Perotti et al. 1991). The MeV bump seen by MISO appears to contain most of the bolometric luminosity of NGC 4151, which cannot be explained by the standard nonthermal pair model, in which less than $\sim 20\%$ of the total power can be radiated in that range (S87; LZ87). To explain that feature, an additional component is required (e.g., a very hot thermal source at low compactness; Sikora & Zbyszewska 1985).

The test of the pair/reflection model will become much more stringent if the observations at greater than 100 keV energies can be improved. For example, the spectral break in hard X-rays obtained by us is roughly the strongest one possible in the nonthermal pair/reflection model under the constraint that the low-energy X-ray power law has a spectral index of $\alpha \gtrsim 0.5$. If a much steeper break is observed in the future (e.g., by *GRO*) *simultaneously* with a spectrum around ~ 10 keV with $\alpha \gtrsim 0.5$, the one-component nonthermal pair model can be rejected.

We thank the referee for valuable suggestions. This research has been supported in part by NASA grants NAG5-1570, NAG5-1813, NAGW-830, NAGW-1284, NAGW-1636, and the Polish State Committee for Scientific Research grants 211879101 and 221129102. P. S. C. would like to acknowledge a NAS Development Visit Grant to Poland, under which this work was begun.

REFERENCES

- Apal'kov, Yu., Babalyan, G., Dekhanov, I., Grebenev, S., Lagunov, I., Pavlinskiy, M., & Sunyaev, R. 1992, in *Frontiers of X-Ray Astronomy*, ed. Y. Tanaka & K. Koyama (Tokyo: Universal Academy Press), 251
- Ayani, K., & Maehara, M. 1991, *PASJ*, 43, L1
- Baity, W. A., Mushotzky, R. F., Worrall, D. M., Rotschild, R. E., Tennant, A. F., & Primini, F. A. 1984, *ApJ*, 279, 555
- Bassani, L., et al. 1986, *ApJ*, 311, 623
- Coppi, P. S. 1992, *MNRAS*, in press
- Coppi, P. S., & Blandford, R. D. 1990, *MNRAS*, 245, 543
- Jourdain, E., et al. 1992, *A&A*, 256, L38 (J92)
- Lightman, A. P., & White, T. R. 1988, *ApJ*, 335, 57
- Lightman, A. P., & Zdziarski, A. A. 1987, *ApJ*, 319, 643 (LZ87)
- Maisack, M., et al. 1989, in *Proc. 23d ESLAB Symp. on Two Topics in X-Ray Astronomy* (ESA SP-296; Paris: ESA), 975
- Maisack, M., & Yaqoob, T. 1991, *A&A*, 249, 25
- Perotti, F., et al. 1990, *ApJ*, 356, 467
- Perotti, F., et al. 1979, *Nature*, 282, 484
- Perotti, F., et al. 1991, *ApJ*, 373, 75
- Pounds, K. A., Nandra, K., Stewart, G. C., George, I. M., & Fabian, A. C. 1990, *Nature*, 344, 132
- Rybicki, G. B., & Lightman, A. P. 1979, *Radiative Processes in Astrophysics* (New York: Wiley)
- Sikora, M., & Zbyszewska, M. 1985, *MNRAS*, 212, 523
- Sunyaev, R. A., & Titarchuk, L. G. 1980, *A&A*, 86, 121 (ST80)
- Svenson, R. 1983, *ApJ*, 270, 300
- . 1987, *MNRAS*, 227, 403 (S87)
- . 1992, in *X-Ray Emission from Active Galactic Nuclei and the Cosmic X-Ray Background*, ed. W. Brinkmann & J. Trümper (MPE Rep. 235; Garching: MPI), 103
- Weaver, K. A., et al. 1992, in *Testing the AGN Paradigm*, ed. S. S. Holt, S. G. Neff, & C. M. Urry (New York: AIP), 192
- White, T. R., Lightman, A. P., & Zdziarski, A. A. 1988, *ApJ*, 331, 939
- Yaqoob, T. 1992, *MNRAS*, in press (Y92)
- Yaqoob, T., & Warwick, R. S. 1991, *MNRAS*, 248, 773
- Zdziarski, A. A. 1980, *Acta Astron.*, 30, 371
- . 1992, in *Testing the AGN Paradigm*, ed. S. S. Holt, S. G. Neff, & C. M. Urry (New York: AIP), 291
- Zdziarski, A. A., Coppi, P. S., & Lamb, D. Q. 1990a, *ApJ*, 357, 149 (Z90a)
- Zdziarski, A. A., Ghisellini, G., George, I. M., Svensson, R., Fabian, A. C., & Done, C. 1990b, *ApJ*, 363, L1 (Z90b)
- Zdziarski, A. A., & Lamb, D. Q. 1986, *ApJ*, 309, L79
- Zdziarski, A. A., & Lightman, A. P. 1985, *ApJ*, 294, L79